Three dimensional laser microfabrication in diamond using a dual adaptive optics system

Richard D. Simmonds,[1] Patrick S. Salter,[1] Alexander Jesacher[2] and Martin J. Booth[1,*]

[1]*Department of Engineering Science, University of Oxford, Parks Road, Oxford, OX1 3PJ, UK*
[2]*Division of Biomedical Physics, Innsbruck Medical University, Müllerstraße 44, 6020 Innsbruck, Austria*
[*]*martin.booth@eng.ox.ac.uk*

Abstract: Femtosecond laser fabrication of controlled three dimensional structures deep in the bulk of diamond is facilitated by a dual adaptive optics system. A deformable mirror is used in parallel with a liquid crystal spatial light modulator to compensate the extreme aberrations caused by the refractive index mismatch between the diamond and the objective immersion medium. It is shown that aberration compensation is essential for the generation of controlled micron-scale features at depths greater than 200 μm, and the dual adaptive optics approach demonstrates increased fabrication efficiency relative to experiments using a single adaptive element.

OCIS codes: (140.3390) Laser materials processing; (090.1000) Aberration compensation; (220.4000) Microstructure fabrication; (220.1920) Diamond machining.

References and links

1. I. Aharonovich, A. D. Greentree, and S. Prawer, "Diamond photonics," Nature Photon. **5,** 397–405 (2011).
2. J. Wrachtrup and F. Jelezko, "Processing quantum information in diamond," J. Phys.: Condens. Matter **18,** S807–S824 (2006).
3. R. P. Mildren and A. Sabella, "Highly efficient diamond Raman laser," Opt. Lett. **34**(18), 2811–2813 (2009).
4. B. A. Fairchild, P. Olivero, S. Rubanov, A. D. Greentree, F. Waldermann, R. A. Taylor, I. Walmsley, J. M. Smith, S. Huntington, B. C. Gibson, D. N. Jamieson, and S. Prawer, "Fabrication of ultrathin single-crystal diamond membranes," Adv. Mater. **20,** 4793–4798 (2008).
5. T. V. Kononenko, M. Meier, M. S. Komlenok, S. M. Pimenov, V. Romano, V. P. Pashinin, and V. I. Konov, "Microstructuring of diamond bulk by ir femtosecond laser pulses," Appl. Phys. A **90,** 645–651 (2008).
6. O. H. Y. Zalloum, M. Parrish, A. Terekhov, and W. Hofmeister, "On femtosecond micromachining of HPHT single-crystal diamond with direct laser writing using tight focusing," Opt. Express **18**(12), 13122–13135 (2010).
7. M. J. Booth, M. A. A. Neil, and T. Wilson, "Aberration correction for confocal imaging in refractive-index-mismatched media," J. Microsc. **192**(2), 90–98 (1998).
8. A. Jesacher and M. J. Booth, "Parallel direct laser writing in three dimensions with spatially dependent aberration correction," Opt. Express **18**(20), 21090–21099 (2010).
9. A. M. Weiner, "Femtosecond pulse shaping using spatial light modulators," Rev. Sci. Instrum. **71**(5), 1929–1960 (2000).
10. M. A. A. Neil, R. Juskaitis, M. J. Booth, T. Wilson, T. Tanaka, and S. Kawata, "Adaptive aberration correction in a two-photon microscope," J. Microsc. **200**(2), 105–108 (2000).
11. D. Oron and Y. Silberberg, "Spatiotemporal coherent control using shaped, temporally focused pulses," Opt. Express **13**(24), 9903–9908 (2005).
12. C. Hsieh, Y. Pu, R. Grange, and D. Psaltis, "Digital phase conjugation of second harmonic radiation emitted by nanoparticles in turbid media," Opt. Express **18**(12), 12283–12290 (2010).
13. M. J. Booth, M. Schwertner, T. Wilson, M. Nakano, Y. Kawata, M. Nakabayashi, and S. Miyata, "Predictive aberration correction for multilayer optical data storage," Appl. Phys. Lett. **88,** 031109 (2006).

#155133 - $15.00 USD Received 22 Sep 2011; revised 17 Oct 2011; accepted 17 Oct 2011; published 10 Nov 2011

14. R. R. Thomson, A. S. Bockelt, E. Ramsay, S. Beecher, A. H. Greenaway, A. K. Kar, and D. T. Reid, "Shaping ultrafast laser inscribed optical waveguides using a deformable mirror," Opt. Express **16**(17), 12786–12793 (2008).
15. C. Mauclair, A. Mermillod-Blondin, N. Huot, E. Audouard, and R. Stoian, "Ultrafast laser writing of homogeneous longitudinal waveguides in glasses using dynamic wavefront correction," Opt. Express **16**(8), 5481–5492 (2008).
16. N. Sanner, N. Huot, E. Audouard, C. Larat, P. Laporte, and J. P. Huignard, "100-khz diffraction-limited femtosecond laser micromachining," Appl. Phys. B **80,** 27–30 (2005).
17. M. Shaw, S. Hall, S. Knox, R. Stevens, and C. Paterson, "Characterization of deformable mirrors for spherical aberration correction in optical sectioning microscopy," Opt. Express **18**(7), 6900–6913 (2010).
18. S. Hu, B. Xu, X. Zhang, J. Hou, J. Wu, and W. Jian, "Double-deformable-mirror adaptive optics system for phase compensation," Appl. Opt. **45**(12), 2638–2642 (2006).
19. M. Booth, T. Wilson, H. Sun, T. Ota, and S. Kawata, "Methods for the characterization of deformable membrane mirrors," Appl. Opt. **44**(24), 5131–5139 (2005).
20. Z. Bor, "Femtosecond-resolution pulse-front distortion measurement by time-of-flight interferometry," Opt. Lett. **14**(16), 862–864 (1989).
21. K. Mecseki, A. P. Kovcs, and Z. L. Horvth, "Measurement of pulse front distortion caused by aberrations using spectral interferometry," in *AIP Conference Proceedings on Light at Extreme Intensities: LEI 2009*, (2010).
22. E. Rittweger, K. Han, S. E. Irvine, C. Eggeling, and S. W. Hell, "Sted microscopy reveals crystal colour centres with nanometric resolution," Nature Photon. **3,** 144–147 (2009).

1. Introduction

Diamond is finding application in a multitude of new research avenues in photonics [1]. For example, a range of colour centres within diamond are useful in quantum information processing [2] or the large Raman gain coefficient provides an attractive medium for Raman lasing [3]. For microfabrication of diamond, either a focussed-ion-beam (FIB) [4] or a tightly focused femtosecond laser [5] may be used for the generation of localised graphitic structures. In this article we describe a system based upon the latter method.

Diamond is transparent at near-infrared wavelengths. However, a tightly focused, ultrashort pulsed laser beam provides the high electric field required for multiphoton absorption and, at powers above a threshold, the local diamond structure is converted into amorphous carbon. The combination of tight spatial focussing and the ultrashort nature of the pulse confines the graphitisation to the focal volume. Such a process has previously been demonstrated in the creation of surface relief structures [6] and graphitic wires within the bulk [5]. However, the fabrication of controlled sub-surface features with diffraction-limited resolution is restricted by spherical aberration caused by the mismatch in the refractive index of the diamond and the immersion medium of the focusing objective lens [7, 8]. This spherical aberration leads to a loss of resolution and power efficiency of fabrication, and increases with focussing depth. This problem is particularly pronounced for fabrication in diamond due to the material's high refractive index (2.4) and the need to use high numerical aperture (NA) optics to obtain the highest resolution. In this paper, we present a dual adaptive optics approach that compensates for the depth dependent aberration, enabling the fabrication of compact features deep within the diamond.

Adaptive optical elements have been utilized in various experimental situations employing ultrafast lasers, such as for manipulation of temporal pulse distribution [9], resolution enhancement in multiphoton microscopes [10, 11] and more recently in imaging through turbid media [12]. An adaptive optical element may be used to correct for depth dependent spherical aberration, by imposing on an incident wavefront a phase profile that is equal and opposite to the aberration introduced by the refractive index mismatch at the sample surface. Previously, both a membrane deformable mirror (DM) [13, 14] and a liquid crystal spatial light modulator (SLM) [8, 15, 16] have been used for aberration correction in laser fabrication systems. A DM provides a continuous phase distortion with large amplitude, but typically has a low number of actuators with which to finely control the mirror shape. In contrast, a SLM benefits from a large

#155133 - $15.00 USD Received 22 Sep 2011; revised 17 Oct 2011; accepted 17 Oct 2011; published 10 Nov 2011

number of pixels, but usually has a maximum modulation depth of 2π radians. To compensate larger aberrations, the phase profile must be wrapped into the range $[0, 2\pi)$ radians. In this paper we apply both a DM and SLM, operating in conjugate planes, to correct for the extreme spherical aberrations generated when using high NA lenses to focus into diamond. Drawing inspiration from "woofer-tweeter" configurations used to correct for atmospheric turbulence in telescopes [18], the DM is used to provide the bulk of the phase compensation, while the SLM is employed adaptively for finer phase adjustment. This allows us to benefit from the advantages of dual adaptive optic devices.

2. Experimental setup

The experimental schematic is shown in Fig. 1. The laser (Newport Spectra Physics Solstice, central wavelength 790nm, 100fs pulse duration, repetition rate 1kHz) pulse energy was controlled using a half-wave plate and a Glan-Taylor polarizer. The beam was expanded onto a phase only liquid crystal SLM (Hamamatsu X10468-02), which was subsequently imaged onto a DM (Imagine Optic MIRAO 52-e) with a pair of achromatic doublets in a $4f$ configuration. Both the SLM and DM were in practice operated at near-normal incidence. The plane of the deformable mirror was mapped onto the pupil of the objective (Olympus 60x 1.4NA oil immersion) with a further $4f$ image system and the beam was focused into the diamond substrate. The diamond was held on a 3D piezo translation stage which enabled 80μm travel in all axes. An LED illuminated widefield microscope was incorporated in order to monitor the fabrication. Initially, the DM was calibrated using the wave-front generator method [19]: with a mirror inserted into the specimen plane of the objective, the focal spot was imaged onto the CCD. Subsequently, a known phase pattern was applied to the SLM, while the DM was adjusted in order to cancel the perturbation to the wavefront and maximise the on-axis focal spot intensity.

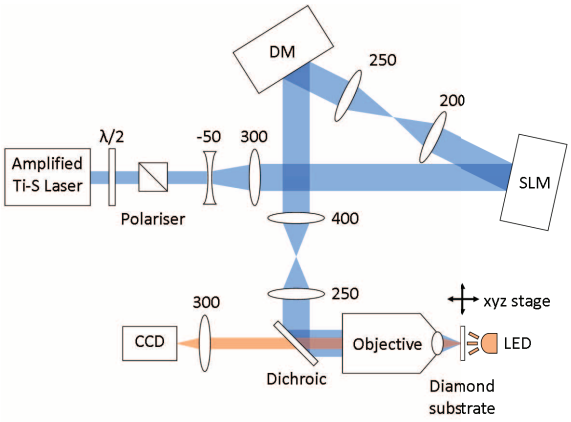

Fig. 1. Experimental schematic. Some intervening optics have been omitted for clarity. The lens focal lengths are in mm.

3. Aberration corrected point fabrication

Graphite point defects were fabricated in the diamond crystal at a series of depths below the surface, as shown in Fig. 2. Fabrication was performed: (i) without any aberration correction applied, i.e. a flat phase profile was displayed on both the SLM and DM; (ii) using a single adaptive optic (the SLM) for feedback correction to compensate the depth dependent spherical aberration while the DM remained flat; and (iii) with dual adaptive optics by assigning a predicted shape for each depth to the DM and again using the SLM for feedback correction,

#155133 - $15.00 USD Received 22 Sep 2011; revised 17 Oct 2011; accepted 17 Oct 2011; published 10 Nov 2011

which was performed as follows. The spherical aberration function was calculated [8] and applied with different amplitudes at a given depth. The amplitude that allowed fabrication with the minimum threshold energy was taken as the optimum correction. The images were obtained with a transmission microscope by observing the features through a polished side facet. Bursts of 50 pulses were used for the fabrication of each feature; this was found to provide highly repeatable results at each depth. In Fig. 2, the threshold pulse energies shown next to each image were measured immediately before the objective. With the dual AO system, the DM was unable to effectively correct aberrations at depths greater than 80 μm in diamond. This is likely related to limitations of the DM calibration routine for large amplitude shapes, and is under further investigation. When using the dual AO system at greater depths, the DM shape was maintained at that for a 50 μm depth and the remainder of the aberration compensated with the SLM.

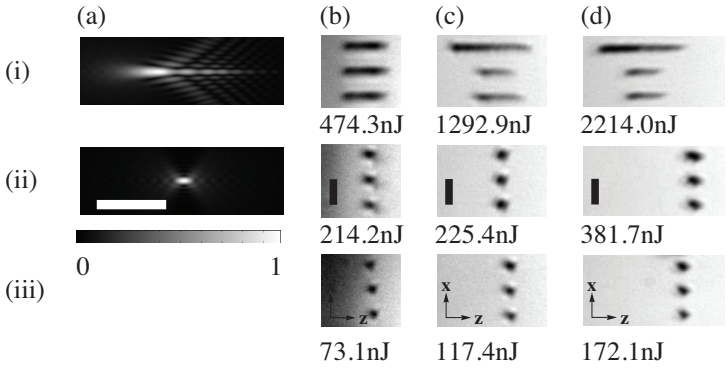

Fig. 2. Simulations of the focal spot intensity distribution at a depth of 40 μm (a) when aberrated (i) and with aberration correction (ii). Images of graphitic defects fabricated at a depth of 40 μm (b), 80 μm (c) and 130 μm (d), using no aberration correction (i), correction using the SLM alone (ii) and correction using a combination of the DM and SLM (iii). The laser propagation direction for both simulation and fabrication was parallel to the positive *z* axis. The scale bars are 5 μm. The pulse energy is shown below each image.

Figure 2 shows axial elongation of the graphitic structures for the uncorrected fabrication beam. This is symptomatic of the focal distortion caused by the refractive index mismatch between the sample and the objective immersion oil, as demonstrated by the simulations of the focal intensity in Fig. 2(a), at depth 40 μm in the diamond (i) and with full aberration compensation (ii). The simulated images are normalized to the same peak intensity at the focus, not the input power, since that was the approximate requirement for experimental fabrication. The focal elongation increases with focussing depth, as seen in row (i). Correspondingly, the focal intensity is reduced and the pulse energy for fabrication must be increased. The groups of three features shown in parts (c) and (d) were each fabricated sequentially from the top feature to the bottom. The shorter length of the second and third features in Fig. 2(i)(c) and (d) is attributed to the presence of the previously created (top) adjacent features affecting the fabrication process through partial obstruction of the illumination cone. By introducing aberration correction to the incident beam, initially using just the SLM, the elongation was reduced resulting in compact structures. The threshold pulse energy was also lower, due to tighter focal confinement. Using both the DM and SLM, the feature size is comparable to the SLM-only correction, but the threshold pulse energy was reduced even further. Although the features fabricated using the dual system appear slightly more compact, it was difficult to determine the exact dimensions as the feature sizes were near to the resolution limit of the microscope. This resolution was also affected by aberrations, as unlike the fabrication system, the microscope did not incorporate adaptive aberration correction. In summary we can conclude that the dual adaptive optics set-

#155133 - $15.00 USD Received 22 Sep 2011; revised 17 Oct 2011; accepted 17 Oct 2011; published 10 Nov 2011

up allows the fabrication of compact features across the tested range of depths with increased power efficiency.

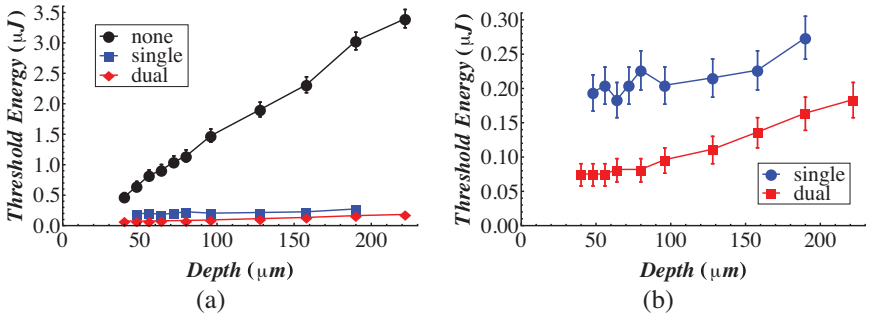

Fig. 3. Graphs comparing the threshold fabrication pulse energy over a range of fabrication depths when using no aberration correction, single (SLM only) aberration correction and dual aberration correction (a) and showing the detail of the two correction options (b). The error bars show the expected range in fabrication threshold energy due to system fluctuations.

Figure 3(a) plots the threshold pulse energy for fabrication as a function of depth in the diamond. Without aberration correction there is an approximately linear increase in the threshold pulse energy as the depth is increased. Both the single and dual adaptive optics approaches also exhibit a roughly linear increase, but the gradient is reduced by a factor > 25 (Fig. 3(b)). Fig. 3(b) allows a closer inspection of the threshold pulse energy dependence on depth for the two adaptive optics approaches. It is clear to see that the power efficiency is improved when using the DM coupled to the SLM: the threshold pulse energy is approximately half that for the SLM-only correction across the entire range.

There are two factors to take into account when considering the greater power efficiency of the dual adaptive optics system. Firstly, the use of phase wrapped pulse correction on the SLM means that the wavefront is corrected modulo 2π radians. As the SLM cannot produce an instant spatial transition from 2π to 0, the phase wrapping is somewhat smoothed. Effectively, this leads to a loss of light at each phase wrapped contour. A second consequence of the SLM phase-wrapping is particular to pulsed lasers. Since the SLM corrects only the wavefront phase and not the full optical path length, in contrast to the continuous distortion of the membrane in the DM, the pulse fronts from spatially distinct regions of the the pupil arrive at the focus at different times [20, 21]. Both effects are exacerbated for large amplitude phase patterns, such as when correcting for greater depths, where more phase wraps are present.

When corrected by the SLM, the pulse front distortion induced by the diamond is estimated to be 36.8fs at the greatest depth tested. For an incident pulse length of 100fs, this is significant and so will affect the multi-photon fabrication efficiency. In combination with light lost at each phase wrap, due to the inability of the SLM to replicate an infinite phase gradient, this causes the increase in threshold energy as the depth increases for single adaptive element correction shown in Fig. 3(b). In using the dual correction, the power efficiency is improved as less phase wrapping is required on the SLM. But, as the fabrication depth increases, so once again does the phase wrapping, resulting in the presented threshold power increase (Fig. 3(b)). Whilst the DM does not suffer from either of the problems of the SLM, when correcting for aberrations at greater depths, a steeper gradient is required for the mirror shape. The limited number of actuators restrict the accuracy with which the DM can generate a prescribed shape and so prevent the DM from performing the necessary correction [17]. For this reason it is necessary to use both adaptive elements in tandem for fabrication at depth in diamond.

#155133 - $15.00 USD Received 22 Sep 2011; revised 17 Oct 2011; accepted 17 Oct 2011; published 10 Nov 2011

4. Fabrication of extended structures

In order to demonstrate 3D fabrication and highlight the necessity of using adaptive elements to compensate the depth dependent aberrations, a series of structures were written into the diamond. Fig. 4 shows fabrication at a constant depth of 80 μm in the diamond (a) with no aberration correction and (b) using the dual AO system. With the laser incident along the *z* direction, graphitic tracks were drawn by translating the sample in the *xy* plane at a speed of 1 μm/s under constant pulsed emission. The pulse energy used was the threshold for burst fabrication at that depth: (a) 1292.9 nJ and (b) 101.5 nJ. When viewing the results in the *xy* plane, both generated structures appear similar except that in the uncorrected fabrication, (Fig. 4(a)), the graphitic tracks are slightly wider and the dots between the sections of the date are absent. However, when viewing the *xz* plane, the contrast is striking. The uncorrected structure (Fig. 4(a)) extends as much as 25 μm above and below the intended fabrication depth whilst the corrected structure (b) has similar dimensions along the optic axis as it does in the plane of fabrication. The view in the *xz* plane also reveals why the dots are missing from the uncorrected structure. The previously written graphitic tracks partially obstruct the focussing cone of the fabrication beam, such that the focal intensity is reduced below threshold. We emphasise that the uncorrected structure was written with the lowest possible (threshold) pulse energy and when the pulse energy was reduced there were no observable features. It is therefore not possible to generate axially confined graphitic tracks in diamond simply by adjusting the power of the writing beam: adaptive compensation for depth dependent aberrations is essential.

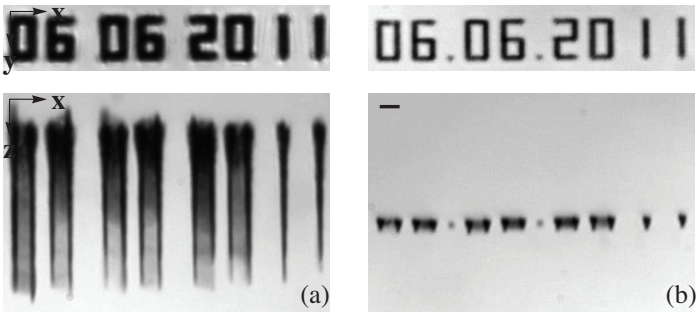

Fig. 4. Top (*xy*) and side (*xz*) view of the date fabricated in diamond at a depth of 80 μm. (a) without aberration correction (b) employing the dual adaptive optics system. The laser beam was incident along the *z* direction. The scale bar represents 5 μm.

Figure 5 shows fabrication in the *xz* plane, both without aberration correction and with the dual correction. The structure was built up by fabricating the deepest structures first so as not to obstruct the incoming beam. During fabrication the SLM phase profile was adjusted according to the focal depth. The writing speed was again 1 μm/s and the pulse energy was kept constant at the fabrication threshold value at the structure's midpoint (80 μm depth). The resultant fabrication confirms how sharp the threshold is, since there was no fabrication at any depth below the midpoint, even under constant pulsed emission. Above the structure midpoint, it was possible to draw graphitic tracks but the axial elongation of the features due to spherical aberration completely obscured any internal structure. When the depth dependent aberration correction was applied, Fig. 5(b), the *xz* structure was successfully fabricated at all depths, maintaining compact dimensions for the features throughout.

#155133 - $15.00 USD Received 22 Sep 2011; revised 17 Oct 2011; accepted 17 Oct 2011; published 10 Nov 2011

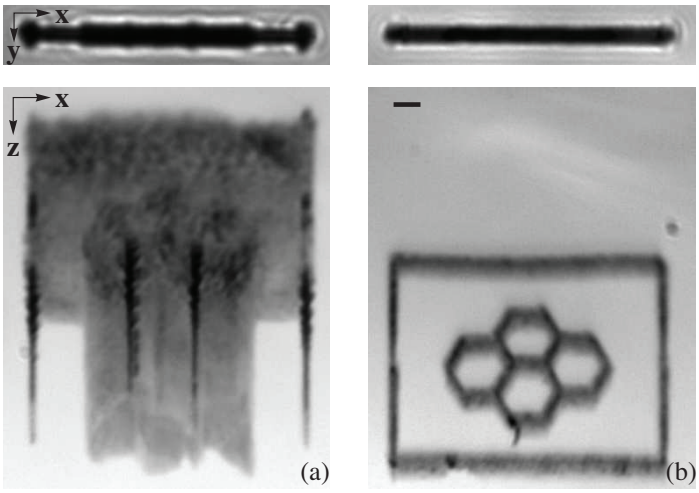

Fig. 5. Top (*xy*) and side (*xz*) view of graphitic structure fabricated in diamond. The midpoint of the structure is at a depth of 80 μm. (a) without aberration correction (b) employing the dual adaptive optics system. The laser beam was incident along the *z* direction. The scale bar represents 5 μm.

5. Conclusion

Compact graphitic structures have been fabricated deep in the bulk of diamond using a femtosecond laser and a dual adaptive optics setup, consisting of a SLM and DM, to correct for depth dependent aberration. Adaptive aberration compensation was shown to be crucial for maintaining controlled fabrication, allowing micron-scale structures to be fabricated down to depths greater than 200 μm. We have shown that adjustment of the writing beam power was not sufficient to generate features that were confined along the optic axis. This was due to the axial extension of the focal spot when aberrated by the refractive index mismatch present at the surface of the diamond substrate. Sharing the load of the aberration between the two adaptive elements led to increased fabrication efficiency compared to using the SLM alone.

The combination of femtosecond laser fabrication with high NA focussing and adaptive optics provides the capability to generate three-dimensional micron-scale structures deep within diamond. Subsequent reactive ion etching of the graphite, as has been demonstrated, for example, in combination with FIB machining [4], leads to the possibility of creation of complex high index contrast devices. These would have many applications in different areas of photonics. These dual adaptive methods also hold great potential benefit for optical microscopy, such as, for example, the observation of color centers in diamond [22].

Acknowledgements

This research was supported by funding from the Engineering and Physical Sciences Research Council, UK (grant numbers EP/H049037/1 and EP/E055818/1) and Jesus College, Oxford.

#155133 - $15.00 USD Received 22 Sep 2011; revised 17 Oct 2011; accepted 17 Oct 2011; published 10 Nov 2011